Letters in Applied NanoBioScience
Open-Access Journal (ISSN: 2284-6808)

Article
Volume 14, Issue 1, 2025, 34
https://doi.org/10.33263/LIANBS141.034

Pharmacoinformatics-based Screening of Phytochemicals from *Euphorbia hirta* Against Corona Virus by Targeting COVID-19 Main Protease

Azar Zochedh [1], Kaliraj Chandran [1], Eswari Chelladurai [1], Amirthavarshini Haribaskar [1], Sureba Sukumaran [1], Thimma Mohan Viswanathan [1], Cibe Chakaravarthy [1], Asath Bahadur Sultan [2,*], Thandavarayan Kathiresan [1,*]

[1] Department of Biotechnology, Kalasalingam Academy of Research and Education, Krishnankoil, Tamil Nadu, India
[2] Condensed Matter Physics Laboratory, Department of Physics, International Research Center, Kalasalingam Academy of Research and Education, Krishnankoil, Tamil Nadu, India
* Correspondence: t.kathiresan@klu.ac.in (T.K.); s.asathbahadur@gmail.com (A.B.S);

Scopus Author ID: 57215079667
Received: 5.08.2023; Accepted: 23.11.2023; Published: 28.09.2024

Abstract: *Euphorbia hirta* is a plant widely distributed throughout much of India and other tropical countries. It has been utilized to treat respiratory disorders because of its analgesic and anti-inflammatory qualities. We investigated about nineteen bioactive phytochemicals in *E.hirta* against the coronavirus using a molecular docking simulation. COVID-19's main protease was chosen as the target protein, and these screened bioactive compounds were docked to it along with a known drug, paclitaxel. The bioactive phytochemicals' docking scores vary from -5.5Kcal/mol to -8.7Kcal/mol against COVID-19 main protease, while the known standard's (CID: 36314) docking score was -8.3 Kcal/mol. The top five compounds ellagic acid (-8.7Kcal/mol), quercetol A (-8.5Kcal/mol), friedelin (-8.4Kcal/mol), taraxerol (-8.3Kcal/mol) and alpha amyrin (-8.3Kcal/mol) based on their binding affinity were further investigated for quantum chemical calculation and drug-likeness prediction. The stability and reactivity were evaluated through DFT, and drug-likeness parameters were assessed through pharmacokinetic studies. These *in silico* findings support the use of *E.hirta* in conventional medicine and the beginning of the development of a novel treatment for COVID-19 through *in vivo* and *in vitro* testing.

Keywords: *Euphorbia hirta*; coronavirus; molecular docking; ADMET; DFT.

© 2024 by the authors. This article is an open-access article distributed under the terms and conditions of the Creative Commons Attribution (CC BY) license (https://creativecommons.org/licenses/by/4.0/).

1. Introduction

The world has recently been dealing with a serious illness known as "Coronavirus disease-2019 (COVID-19)" that has had an impact on the economics and health of the entire world [1]. A respiratory illness called COVID-19 has the potential to result in death [2,3], as well as fever, malaise, dry cough, and pneumonia. No effective medicine has yet been developed to treat or prevent this infection [4]. Scientists worldwide are working to develop an effective medicine for this urgent problem [5,6]. Adefovir, Foscarnet, Tenofovir, Sofosbuvir, Uprifosbuvir, and Remdesivir are examples of potent antiviral medications based on phosphorus amide and phosphate with pyrazin and imidazole rings in their structures that have been studied for the treatment of COVID-19 [7]. Remdesivir (GS-5734), one of these molecules, was thought to be the most promising medication that might be used to treat

COVID-19 [8]. With broad-spectrum antiviral action against pneumonia viruses, paramyxoviruses, filoviruses, and coronaviruses [8,9], this substance is a mono-phosphoramidate prodrug. Clinical trials are currently being conducted to determine the full efficacy of this prodrug in humans [10,11]. Recent research has shown that the medications described above inhibit the major viral protease, which is how they work. The most promising pharmacological target against coronaviruses is, in fact, the ability of the major protease (Mpro) to be inhibited [12-16]. Molecular docking approaches, widely utilized in contemporary drug design, investigate the ligand conformations taken within the binding sites of macromolecular targets [17,18]. These procedures are logically successful in predicting binding affinity and have shown promising potential in facilitating drug design [19]. The family Euphorbiaceae is exceptional since it includes well-known plants effective against several ailments. This genus contains a wide range of chemical species with numerous causes of structural diversity. Many of these plants, including Amla (Emblica officinalis), Bhoiamli (Phyllanthus fractus), Arendmul (Racinus communis), Dudhi (*Euphorbia hirta*), and Ratidudhi (Euphorbia thymifolia), among others, have medicinal value in the management of certain chronic diseases, including diabetes, hemorrhoids, asthma inflammation, etc. [20]. Complementary and alternative medicine (CAM) encompasses various conventional and cutting-edge methods for treating or preventing disease. A few drugs derived from conventional indigenous plants have been used by a traditional Indian medical system to treat liver illness [21]. In the Gujarati language, the *Euphorbia hirta L* (Euphorbiaceae), also known as dudheli, is a plant that grows profusely throughout most of India and other tropical nations, particularly along highways and in wastelands [22,23]. The weed plant *E. hirta* is widely distributed in open grasslands and along roadsides. The leaves are opposite, elliptical or oblong, and have a serrated border. It is a tall, slender shrub occasionally found dispersed throughout the soil. Smaller cymes serve as the flowers [24]. After cutting the stem, the milky white fluid is gone [25,26]. Due to its analgesic and anti-inflammatory properties, *E.hirta* has historically been used to treat respiratory conditions such as asthma, bronchitis, and hay fever [27]. Hence, in this work, due to the need to discover new inhibitors and factors affecting Mpro inhibition, an attempt will be made to introduce new inhibitors based on bioactive compounds of *E.hirta* with higher COVID-19 Mpro inhibition potential than current acceptable drugs by molecular docking method and to analyze the stability and reactivity of the phytochemicals based on HOMO and LUMO gaps and also to evaluate the drug-likeness profile of the phytochemicals based on physiochemical and ADMET properties.

2. Materials and Methods

2.1. Protein retrieval and processing.

The crystal structure of the COVID-19 main protease (PDB ID: 6LU7) was retrieved from the RCSB Protein Data Bank server (http://www.rcsb.org/pdb) [28]. Initially, the downloaded target protein was processed through the BIOVIA Discovery Studio 2021 client by adding the lost residues and side chains. Then, the water molecules, hetatms, and unwanted ligands were cleared from the target protein's structure and saved in ".pdb" for docking simulation.

2.2. Bioactive compounds retrieval.

Dr.Duke's Phytochemical and Ethnobotanical database was utilized to retrieve the bioactive constituents present in Euphorbia *hirta* (https://phytochem.nal.usda.gov). We screened around 19 bioactive phytochemicals from *Euphorbia hirta* and retrieved their 3D structure from the PubChem database (https://pubchem.ncbi.nlm.nih.gov/). A known COVID-19 drug was utilized as standard during the docking studies along with the bioactive phytochemicals.

2.3. Active site prediction.

The ideal pockets in the active sites were identified through the CASTp (Computed Atlas of Surface Topography of Proteins) online server (http://sts.bioe.uic.edu/castp/index.html?3trg). The target protein's active site permits the ligand to bind and perform a reaction. In the CASTp server, the PDB ID of the target protein was given as an input, and the output appears with numerous ideal pockets at the active chains of the target protein.

2.4. Molecular docking simulation.

The widely utilized in-silico technique in drug design development is molecular docking. In this study, molecular docking was performed using PyRx 0.8 software [29]. The ligands (bioactive phytochemicals and known COVID-19 drug) and target protein (PDB ID: 6LU7) were loaded on the graphical window. Then, the grid box was made on the active region of the target protein, and molecular docking was computed. Then, docking scores were analyzed. From the output file of molecular docking, the visualization of protein and ligands was analyzed. The top five compounds with higher docking scores were investigated for the protein-ligand interactions, and the interaction images were demonstrated through the BIOVIA Discovery Studio 2021 client tool.

2.5. Density functional theory.

Density function theory (DFT) was computed to investigate the electronic states of atoms and molecules based on three-dimensional electron density structure [30]. The electronic effect is an important factor for a drug-like compound's biological activity. Gaussian 09W software optimized the lead compounds and computed frontier molecular orbitals through DFT/B3LYP with a 6-311 G basis set [31]. The selected bioactive compounds with top binding affinity were optimized and computed for frontier molecular orbital (FMO) energies based on the energy values depending on the difference between the lowest unoccupied molecular orbital and the highest occupied molecular orbital.

2.6. ADMET profile.

The pharmacokinetic evaluation was performed on the online server pkCSM for the selected bioactive compounds (http://biosig.unimelb.edu.au/pkcsm/prediction) [32]. The pharmacokinetic prediction for the selected bioactive compounds based on the docking score was evaluated based on the physiochemical, absorption, distribution, metabolism, excretion, and toxicity properties.

3. Results

3.1. Active site prediction.

Utilizing the CASTp server, ideal binding pockets in the active site regions were predicted for the target protein COVID-19 main protease. The CASTp analysis will be useful in predicting more potential ideal pockets in the active site of the COVID-19 main protease target protein. A total number of 37 pockets were analyzed, out of which an ideal binding pocket with a surface area of 351.125Å was designated as an active site region and was demonstrated in Figure 1. These ideal pockets in the target protein were applied to build the grid box during molecular docking. When performing the molecular docking simulation at the ideal binding pockets of the active site region, the resultant binding affinity may be robust, and the molecular docking scores will be higher for the bioactive ligands.

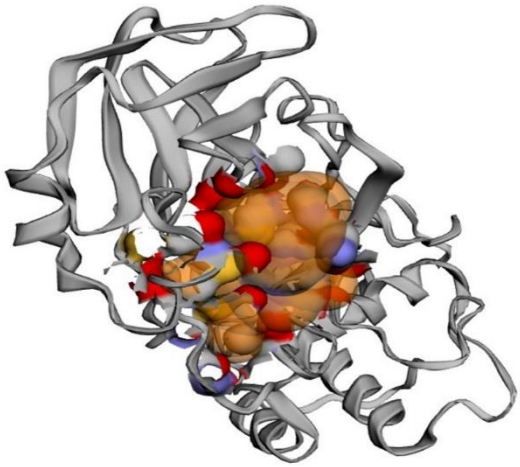

Figure 1. Predicted active site region of the target protein COVID-19 main protease.

3.2. Molecular docking simulation.

The binding capability of the 19 bioactive compounds from *Euphorbia hirta* against the COVID-19 main protease (PDB ID: 6LU7) target protein. In this current docking investigation, a known drug paclitaxel (CID: 36314) was utilized as standard due to its previously accounted anti-COVID potential [32]. The docking scores of the docked constituents of E.hirta against the 6LU7 target were observed to be between the range of -5.5Kcal/mol to -8.7Kcal/mol, and Table 1 represents the binding affinity of the nineteen phytochemicals along with paclitaxel against the target protein. The phytochemicals ellagic acid, quercetol A, friedelin, taraxerol, and alpha amyrin showed the highest binding affinity among the nineteen bioactive constituents with the docking scores of -8.7, -8.5, -8.4, -8.3 and -8.3Kcal/mol. The lowest docking score was observed with the phytochemicals gallic acid and inositol, with a binding affinity of -5.5Kcal/mol.

Further, the binding affinity of known standard paclitaxel was -8.3Kcal/mol, and the binding scores of phytochemicals of E.hirta, ellagic acid, quercetol A, and friedelin exhibited higher binding potential with the scores -8.7, -8.5 and -8.4Kcal/mol when compared to known drug and also the bioactive compounds taraxerol and alpha amyrin showed same binding affinity as of standard. These phytochemicals with the COVID-19 main protease (PDB ID: 6LU7) target showed great binding potential. Therefore, these phytochemicals could be a better contender for the 6LU7 target to prevent coronavirus.

Table 1. Docking scores of bioactive constituents of *Euphorbia hirta* against target protein.

S. No.	PubChem ID	Phytochemicals	Binding Affinity (Kcal/mol)
1	73170	Alpha-Amyrin	-8.3
2	73145	Beta-Amyrin	-7.9
3	72326	Betulin	-7.3
4	689043	Caffeic-Acid	-5.7
5	173183	Campesterol	-7.7
6	92110	Cycloartenol	-6.9
7	5281855	Ellagic-Acid	-8.7
8	445858	Ferulic-Acid	-5.6
9	91472	Friedelin	-8.4
10	370	Gallic-Acid	-5.5
11	892	Inositol	-5.5
12	5280863	Kaempferol	-7.8
13	440833	Leucocyanidol	-7.1
14	637542	P-Coumaric-Acid	-5.8
15	5280343	Quercetin	-7.2
16	44257151	Quercetol A	-8.5
17	5281691	Rhamnetin	-7.3
18	16129778	Tannic-Acid	-7.8
19	92097	Taraxerol	-8.3
20	36314	Paclitaxel (Standard)	-8.3

The interaction of target protein COVID-19 main protease (PDB ID: 6LU7) with the bioactive phytochemicals friedelin, ellagic acid, taraxerol, alpha amyrin, and quercetol A were represented in Figure 2 to Figure 6. Friedelin with the target COVID-19 main protease exhibited hydrogen bond and hydrophobic bond interactions with the bond category of three donor conventional hydrogen bonds with amino residues ARG131 and LYS137 (2) at 2.99176Å, 2.55637Å and 2.64814Å and four alkyl hydrophobic interactions with LEU286, LEU287 (2) and MET276 at 5.4268Å, 5.34562Å, 4.55234Å and 4.11195Å bond distances.

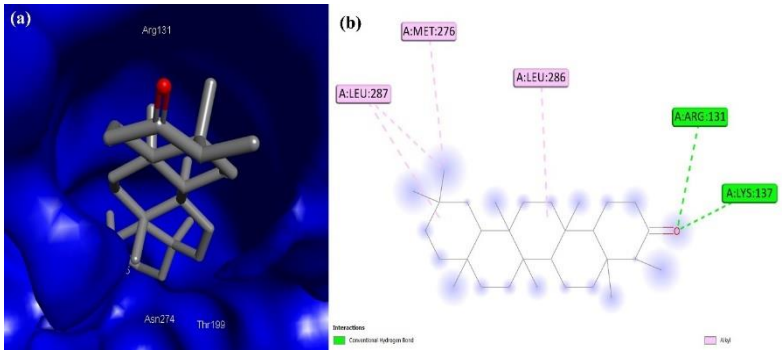

Figure 2. (a) Binding of friedelin at the receptor region of a target protein. **(b)** 2D interaction of friedelin against target protein with interaction types.

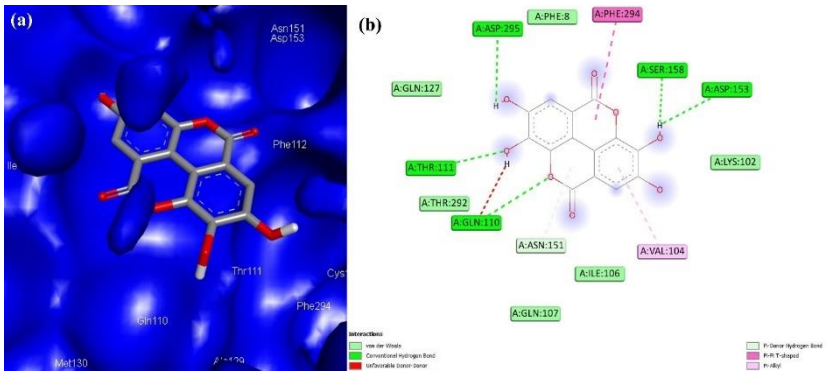

Figure 3. (a) Binding of ellagic acid at the receptor region of target protein. **(b)** 2D interaction of ellagic acid against target protein with interaction types.

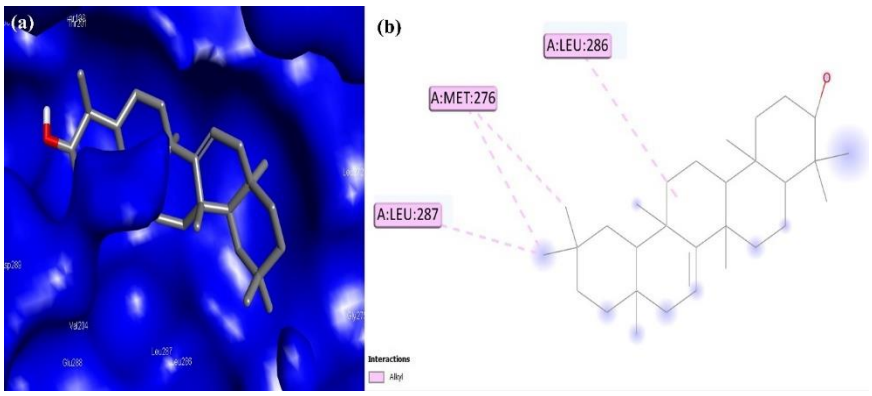

Figure 4. (a) Binding of taraxerol at the receptor region of a target protein. **(b)** 2D interaction of taraxerol against target protein with interaction types.

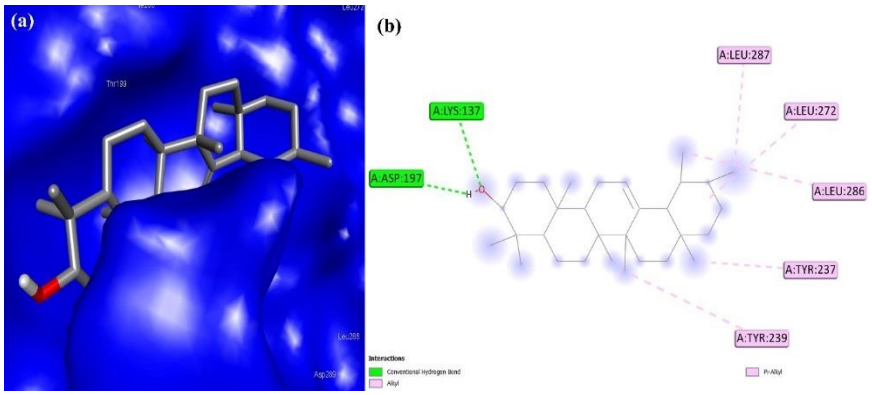

Figure 5. (a) Binding of alpha amyrin at the receptor region of a target protein. **(b)** 2D interaction of alpha amyrin against target protein with interaction types.

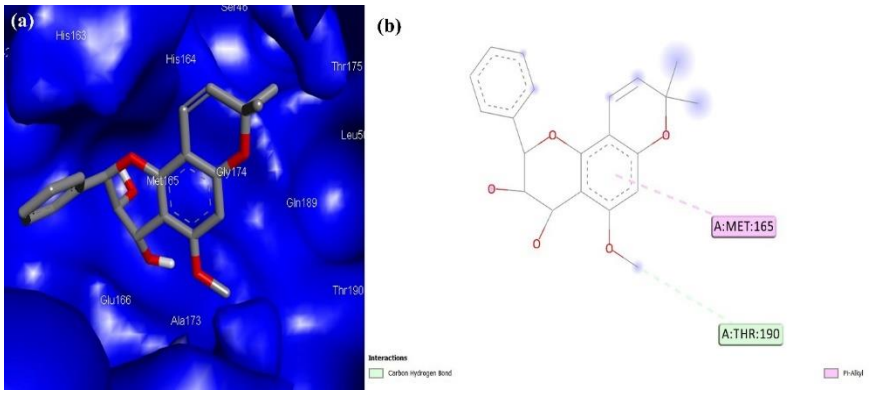

Figure 6. (a) Binding of quercetol A at the receptor region of a target protein. **(b)** 2D interaction of quercetol A against target protein with interaction types.

The lead compound ellagic acid with target protein showed two donor and three acceptor conventional hydrogen bond interactions along with one Pi-donor hydrogen bond interaction with amino residues (distance) of GLN110 (3.1494Å), THR111 (3.20415Å), ASP153 (2.92231Å), SER158 (2.57067Å), ASP295 (2.50224Å) and ASN151 (3.8492Å). Taraxerol against the 6LU7 formed four alkyl hydrophobic bond interactions with LEU286, MET276 (2), and LEU287 at 4.88481Å, 4.222022Å, 4.29459Å and 3.9322Å respectively. Alpha amyrin with target protein formed one donor and one acceptor hydrogen bond interaction with LYS137, ASP197 and LEU272 with three alkyl and two Pi-alkyl hydrophobic interactions with amino residues LYS137, ASP197, LEU272, LEU286, LEU287, TYR237 and TYR239 at bond distances 1.96413Å, 2.37442Å, 5.39865Å, 4.9517Å, 4.15888Å, 5.34614Å and 4.9374Å. The compound quercetol A against the protein of the target formed a single acceptor carbon-

hydrogen bond with THR190 (3.72703Å) and one Pi-Alkyl hydrophobic bond interaction with MET165 amino residue at a bond distance of 4.76211Å. The type of hydrogen bond, bond category, and distance of the bond play a vital role in molecular docking. The top five phytochemicals with a binding score greater than -8Kcal/mol showed greater binding interactions and exhibited hydrogen and hydrophobic bond interactions.

3.3. Frontier molecular orbitals based on DFT.

The investigation of molecular orbitals governs by what means a compound relates to various species. The lowest unoccupied molecular orbital (LUMO) and highest occupied molecular orbital (HOMO) were evaluated through the DFT method using the B3LYP/6-311 G basis set. The obtained LUMO and HOMO values were further used to evaluate the energy gap between them. HOMO is a nucleophile that donates electrons to LUMO, whereas LUMO is an electrophile that accepts electrons from HOMO [33]. The molecule's stability can also be evaluated through the frontier molecular orbital investigation. The lesser energy gap molecules were considered softer, highly polarizable, and had better chemical reactivity, whereas the higher energy gap molecules were considered highly stable and had good chemical hardness [34]. From the calculated energy gap, electron affinity (A), ionization potential (I), chemical potential (μ), electronegativity (χ), softness (S), global hardness (η), and electrophilicity index (ω) can be evaluated for the top five phytochemicals depending on Koopman's theorem. Table 2 depicts the calculated values of the phytochemicals based on FMO, and Figure 7 to 11 represents the HOMO and LUMO areas of the phytochemicals. The evaluated LUMO and HOMO gap i.e., the energy gap (ΔE=ELUMO-EHOMO) of the top five phytochemicals are 5.95221eV (friedelin), 4.29776eV (ellagic acid), 7.25155eV (taraxerol), 7.18434eV (alpha amyrin) and 4.93913 eV (quercetol A).

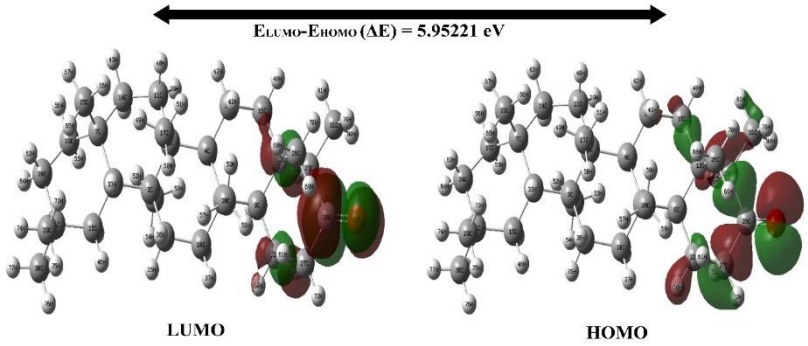

Figure 7. The computed FMO and energy value of friedelin using DFT/B3LYP with 6-311 G basis set.

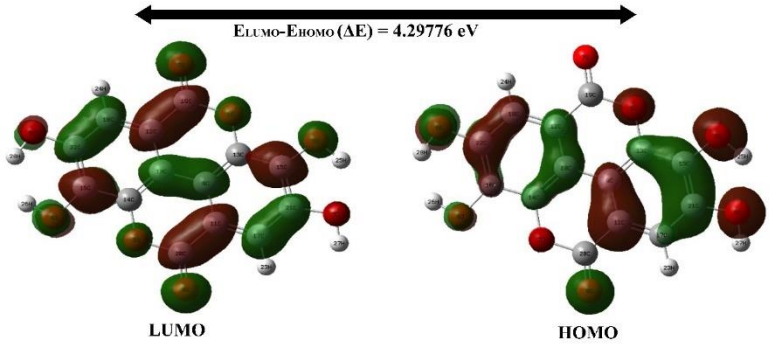

Figure 8. The computed FMO and energy value of ellagic acid using DFT/B3LYP with 6-311 G basis set.

The electron affinity (A) and ionization potential (I) were the negative energies of LUMO and HOMO, where A = ELUMO and I = EHOMO. The electronegativity (χ) was

calculated by χ= (I+A)/2, and its negative value represents the chemical potential (μ) and the chemical hardness (η) was evaluated by η = (I-A)/2. Its inverse represents the chemical softness S = 1/η. The electrophilicity index was calculated by $\omega = \mu 2/2\eta$, and its inverse was nucleophilicity (N), N = 1/ω.

From the calculated energy gap values, it was confirmed that the lower energy value of ellagic acid with 4.29776eV showed better binding affinity (-8.7Kcal/mol) when compared to other top phytochemicals and the phytochemicals taraxerol and alpha amyrin exhibited higher energy values greater than 7eV that showed their good structural stability but less chemical reactivity. These computed energy values have proven that the molecules with lower energy possess higher binding affinities against the target protein.

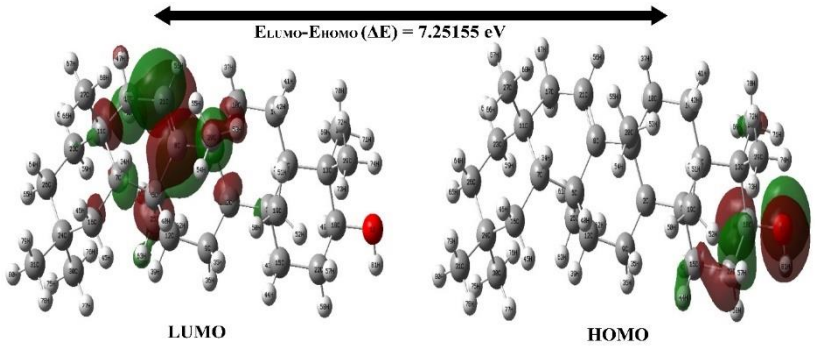

Figure 9. The computed FMO and energy value of taraxerol using DFT/B3LYP with 6-311 G basis set.

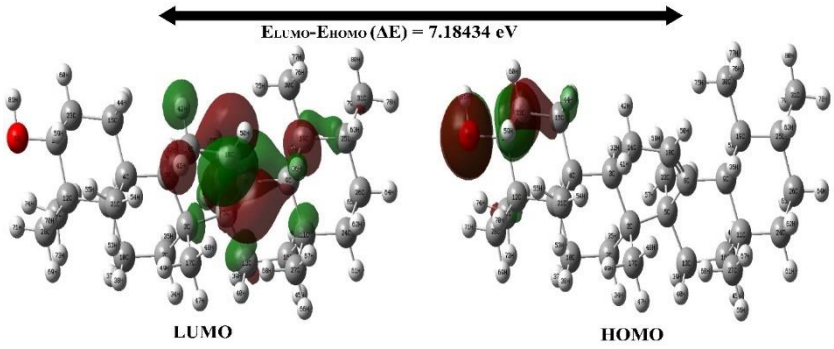

F**igure 10.** The computed FMO and energy value of alpha amyrin using DFT/B3LYP with 6-311 G basis set.

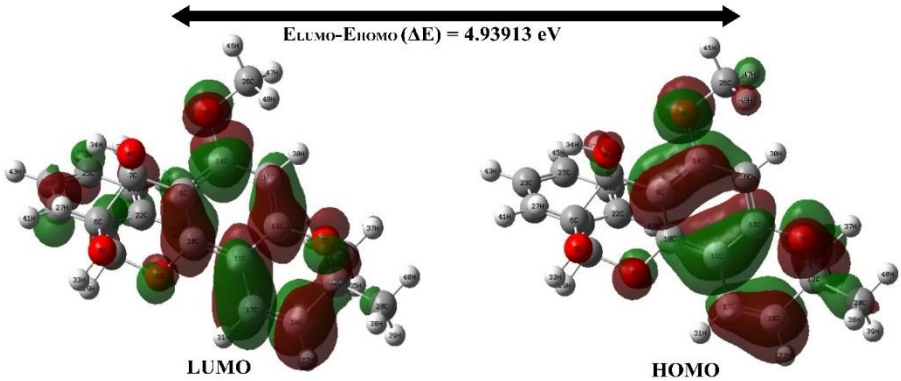

F**igure 11.** The computed FMO and energy value of quercetol A using DFT/B3LYP with 6-311 G basis set.

Table 2. Evaluated FMO values of the top five phytochemicals of *Euphorbia hirta.*

Parameters (eV)	Friedelin	Ellagic acid	Taraxerol	Alpha amyrin	Quercetol A
E_{LUMO}	2.40603	0.68219	3.62836	3.55870	2.04085
E_{HOMO}	-3.54618	-3.61557	-3.62319	-3.62564	-2.89828
Δ(ELUMO - EHOMO)	5.95221	4.29776	7.25155	7.18434	4.93913
Electron Affinity (A)	-2.40603	-0.68219	-3.62836	-3.55870	-2.04085
Ionization Potential (I)	3.54618	3.61557	3.62319	3.62564	2.89828

Parameters (eV)	Friedelin	Ellagic acid	Taraxerol	Alpha amyrin	Quercetol A
Electronegativity (χ)	0.56789	1.46669	-0.00259	0.03347	0.428715
Chemical Potential (μ)	-0.56789	-1.46669	0.00259	-0.03347	-0.428715
Chemical Hardness (η)	2.97611	2.14888	3.625775	3.59217	2.46957
Chemical softness (S)	0.33601	0.46536	0.27581	0.27838	0.40493
Electrophilicity Index(ω)	0.05418	0.50054	0.000000924	0.000156	0.037212
Nucleophilicity (N)	18.4569	1.99784	1082251.08	6410.256	26.8731

3.4. ADME properties.

The drug-likeness properties of the top five phytochemicals were evaluated utilizing the online server pkCSM. In drug discovery, the physiochemical parameters play a vital role in analyzing whether the drug molecule satisfies the five rules of Lipinski. Lipinski's rule is the chief factor in oral drug development. A molecule can be well thought out as an oral drug only if it satisfies all of Lipinski's rules without violation or with one violation as a maximum. Table 3 depicts the obtained physiochemical parameters of the top five phytochemicals of the *E.hirta* plant. According to the 'Lipinski's rule, the molecular weight should be less than 500Da, the H-Bond donor should be 5 or fewer, and the number of rotatable bonds and H-Bond acceptor should be 10 or fewer. There can only be one rule broken at a time. Molecular weights of friedelin, taraxerol, and alpha amyrin possess the same molecular weight of 426.729 Da, which is the highest among the top five phytochemicals, followed by quercetol A with 354.402 Da and ellagic acid with 302.194 Da.

Similarly, the surface area of the top five compounds: friedelin, ellagic acid, taraxerol, alpha amyrin, and quercetol A, are 192.455Å^2, 118.565Å^2, 192.398Å^2, 192.398Å^2 and 192.455Å^2 respectively. None of the top five phytochemicals have violated Lipinski's rules. Therefore, top-hit phytochemicals could be considered for oral medications. The compound ellagic acid possesses the highest water solubility range of -3.181, followed by quercetol A with -3.638, and the least water solubility was accounted for by alpha amyrin with -6.499. The $CaCO_2$ permeability was accounted for between the values of 0.335 to 1.266, as the highest $CaCO_2$ permeability was predicted for friedelin and the lowest for ellagic acid. This shows that ellagic acid has the lowest $CaCO_2$ permeability compared to other top phytochemicals. The human intestinal absorption was at the percentage range between 86.684 to 98.736 %, which confirms that all the top five phytochemicals possess good intestinal absorbance and the skin permeability range of all the compounds lies around -2, which also confirms that all phytochemicals likely skin permeable as their range lies less than -2.5. Among five, ellagic acid and quercetol A were P-glycoprotein substrates, and the other three were P-glycoprotein I and II inhibitors. The steady-state volume distribution (VDss) was greater for quercetol A with the range of 0.408, and the least was predicted for friedelin with -0.272. Generally, VDss was considered low when its range fell under 0.71; therefore, it shows that all the phytochemicals possess low VDss value. Alpha amyrin, taraxerol, and friedelin readily cross the blood-brain barrier, whereas other phytochemicals poorly penetrate the blood-brain barrier. Except for ellagic acid, all other phytochemicals penetrate through CNS, as the phytochemicals with a range less than -3 were considered unable to penetrate CNS. None of the phytochemicals were CYP2D6 substrate, CYP2D6 inhibitor, or CYP3A4 inhibitor, except ellagic acid; all others were CYP3A4 substrate. Only ellagic acid and quercetol A were the inhibitors of CYP1A2, and the inhibition of CYP2C19 and CYP2C9 was found only in quercetol A. The total clearance value of the five phytochemicals falls between the range of -0.04 to 0.537, with the highest range predicted for ellagic acid and lowest for friedelin, and all the phytochemicals were not renal OCT2 substrates. This physiochemical and ADMET evaluation exhibited that

the top five phytochemicals possess good drug-likeness properties without violating Lipinski's rule.

Table 3. Predicted pharmacokinetic parameters of top five phytochemicals.

Descriptors	Friedelin	Quercetol A	Ellagic Acid	Alpha Amyrin	Taraxerol
Molecular weight	426.729	354.402	302.194	426.729	426.729
No of rotatable bonds	0	2	0	0	0
No of acceptors	1	5	8	1	1
No of donors	0	2	4	1	1
Surface area	192.455	192.455	118.565	192.398	192.398
Water solubility	-5.514	-3.638	-3.181	-6.499	-6.31
Caco2 permeability	1.266	1.146	0.335	1.227	1.212
Intestinal absorption (human)	98.736	94.07	86.684	94.062	94.036
Skin permeability	-2.605	-2.766	-2.735	-2.814	-2.788
P-glycoprotein substrate	No	Yes	Yes	No	No
P-glycoprotein I inhibitor	Yes	No	No	Yes	Yes
P-glycoprotein II inhibitor	Yes	No	No	Yes	Yes
VDss (human)	-0.272	0.408	0.375	0.266	0.206
BBB permeability	0.72	-0.066	-1.272	0.674	0.678
CNS permeability	-1.555	-2.072	-3.533	-1.773	-1.891
CYP2D6 substrate	No	No	No	No	No
CYP3A4 substrate	Yes	Yes	No	Yes	Yes
CYP1A2 inhibitor	No	Yes	Yes	No	No
CYP2C19 inhibitor	No	Yes	No	No	No
CYP2C9 inhibitor	No	Yes	No	No	No
CYP2D6 inhibitor	No	No	No	No	No
CYP3A4 inhibitor	No	No	No	No	No
Total Clearance	-0.04	0.058	0.537	0.119	-0.081
Renal OCT2 substrate	No	No	No	No	No

3.5. Toxicity analysis.

The predicted toxicity parameters of the top five phytochemicals are represented in Table 4. The top five phytochemicals were non-toxic to AMES toxicity. The maximum tolerated dosage for the phytochemicals in humans lies between -0.135 and 0.476, with the highest dosage predicted for ellagic acid. None of the phytochemicals were hERG I inhibitors, except for ellagic acid, all other phytochemicals were hERG II inhibitors. The LD50 values of friedelin, quercetol A, ellagic acid, alpha amyrin, and taraxerol were 2.64, 2.128, 2.399, 2.467, and 2.386 and LOAEL values were 0.909, 2, 2.698, 0.856 and 0.808 respectively. The top phytochemicals show no hepatotoxicity and skin sensitization. Therefore, all these phytochemicals were -toxic, showing a better safety profile for further developing the drug against the coronavirus.

Table 4. Toxicity parameters of the top five phytochemicals predicted through pkCSM.

Toxicity Parameters	Friedelin	Quercetol A	Ellagic Acid	Alpha Amyrin	Taraxerol
AMES toxicity	No	No	No	No	No
Max. tolerated dose (human)	-0.213	-0.135	0.476	-0.571	-0.623
hERG I inhibitor	No	No	No	No	No
hERG II inhibitor	Yes	Yes	No	Yes	Yes
Oral Rat Acute Toxicity (LD50)	2.64	2.128	2.399	2.467	2.386
Oral Rat Chronic Toxicity (LOAEL)	0.909	2	2.698	0.856	0.808
Hepatotoxicity	No	No	No	No	No
Skin Sensitisation	No	No	No	No	No

4. Discussion

The main purpose of this study is to identify and evaluate several parameters of the bioactive phytochemicals existing in *Euphorbia hirta* through molecular docking, density

function theory, and pharmacokinetic approaches. Screening phytochemicals is an initial process to recognize the biologically active phytochemicals present in that particular plant. In *Euphorbia hirta, a* total of nineteen bioactive phytochemicals were analyzed. In this case, these phytochemicals were utilized to evaluate the inhibition mechanism against COVID-19 main protease. Due to this study, we were able to focus the efforts of researchers in the field of determining the function of the *Euphorbia hirta* against coronavirus. By examining the binding affinity and interaction profile of these bioactive phytochemicals, we can forecast several possible strategies as pharmaceutical drugs. The bond distance intermediate to the amino residue and the docked phytochemicals, the category of interacted bond, the hydrogen and hydrophobic interactions, and the binding scores of the bioactive phytochemicals against the targeted protein COVID-19 main protease at its ideal binding pockets all play key roles in the efficient binding of the phytochemicals and corona associated protein. The top compounds with higher binding scores were visualized for protein-ligand interactions, and those five compounds exhibited hydrogen bond and hydrophobic bonds, representing their better binding at the receptor regions of the target protein [35]. The density function theory represents the chemical reactivity and the structural stability of the top phytochemicals with the B3LYP/STO-3G basis set. The LUMO and HOMO energy gaps of the top five phytochemicals were computed between the range of 4.29776eV to 7.25155eV that confirms that the phytochemicals with low energy gap possess better chemical reactivity [36], as the ellagic acid with lower energy of 4.29776eV possesses highest binding affinity of -8.7Kcal/mol. Predicting how various phytochemicals will interact with the human body can be made easier by being aware of their biological activities [37]. Predicting bioactivity involves tracking absorption, distribution, metabolism, and excretion, all of which are ADME properties. Investigating the bioactive compound's efficacy against COVID-19's main protease is important. The process of absorption is where the supplied phytochemicals are first transferred. Friedelin has been found to have a greater intestinal absorption in this situation, making it simpler to absorb via the digestive system (GI tract). Our information makes it easier to determine how well phytochemicals are absorbed through the GI system. When a medication is absorbed, it must go through a distribution process that entails the permeability of the molecule and characterizes the compound's whole bioactivity. Only a tiny percentage of the drug molecules provided for dispersion reach the target fully; the majority disintegrate before they do. The three bioactive compounds (alpha amyrin, taraxerol, and friedelin) penetrate through the blood-brain barrier, whereas the remaining two poorly penetrate BBB, and except ellagic acid, all other compounds possess CNS permeability. These records offer a solid place to start for predicting bioactivity, but further research, including clinical trials, is required to represent the procedure clearly.

Additionally, an in vivo excretion study helps us more effectively describe the pharmacokinetic features of these phytochemicals. The ellagic acid appears to have a total clearance of 0.537, which is more than enough, and the renal OCT2 exhibits no impact on the top five phytochemicals. Understanding bioactivity is fundamental, but it's also critical to comprehend side effects and toxicity characteristics when it comes to approving a medication. There is a common belief that herbal remedies are generally linked to more serious side effects. Contrarily, herbal remedies are substantially more efficient and less hazardous than synthetic pharmaceuticals [38]. This research shows that all of the top five phytochemicals tested 'don't cause hepatotoxicity and skin irritation, and for all the phytochemicals AMES toxicity values seem to be satisfactory, and the LD50 results appear to be adequate compared to other results. There is no hERG I inhibitor, except for ellagic acid, all others were hERG II inhibitors.

Knowing the top five phytochemical toxicological characteristics allows us to employ them in ways that interact with the human body for the treatment of coronavirus.

5. Conclusions

The findings of the present study suggested that all of the bioactive phytochemicals from the *Euphorbia hirta* had excellent binding ability at the ideal pockets of COVID-19 main protease, suggesting that these phytochemicals may be able to prevent coronavirus. The binding of the bioactive compounds against the target protein could inhibit the activity of COVID-19's main protease. From the screened nineteen bioactive compounds, five of them (friedelin, quercetol A, ellagic acid, alpha amyrin, and taraxerol) exhibited greater binding scores (>8Kcal/mol) against target protein, and ellagic acid showed the highest binding affinity of -8.7Kcal/mol. According to FMOs research, the bioactivity of the top five phytochemicals is influenced by several characteristics, including the molecular reactivity, kinetic stability, and intramolecular charge transfer of the molecule. The stability and reactivity were assessed using band gap energy values between LUMO and HOMO. Further testing of the top five compound's pharmacokinetics data revealed that they might make suitable medication candidates because of their low or non-existent toxicity to humans. To learn more about their actions and effectiveness against COVID-19, more *in vivo* and *in vitro* investigations are required.

Funding

This research was funded by a Grant-aid from the Department of Biotechnology (DBT), Ministry of Science and Technology, India [BT/PR44695/NER/95/1880/2021].

Acknowledgments

The authors acknowledge Dr.S.Athimoolam, Department of Physics, University College of Engineering, Anna University, Nagercoil, for helping us utilize the Gaussian 09 Program.

Conflicts of Interest

The authors have no relevant financial or non-financial interests to disclose.

References

1. Tandon, P.N. COVID-19: Impact on health of people & wealth of nations. *Indian J. Med. Res.* **2020**, *151*, 121-123, https://doi.org/10.4103%2Fijmr.IJMR_664_20.
2. Huang, C.; Wang, Y.; Li, X.; Ren, L.; Zhao, J.; Hu, Y.; Zhang, L.; Fan, G.; Xu, J.; Gu, X.; Cheng, Z.; Yu, T.; Xia, J.; Wei, Y.; Wu, W.; Xie, X.; Yin, W.; Li, H.; Liu, M.; Xiao, Y.; Gao, H.; Guo, L.; Liu, M.; Xiao, Y.; Gao, H.; Guo, L.; Xie, J.; Wang, G.; Jiang, R.; Gao, Z.; Jin, Q.; Wang, J.; Cao, B. Clinical features of patients infected with 2019 novel coronavirus in Wuhan, China. *Lancet* **2020**, *395*, 497-506, https://doi.org/10.1016/S0140-6736(20)30183-5.
3. Zhu, N.; Zhang, D.; Wang, W.; Li, X.; Yang, B.; Song, J.; Zhao, X.; Huang, B.; Shi, W.; Lu, R.; Niu, P.; Zhan, F.; Ma, X.; Wang, D.; Xu, W.; Wu, G.; Gao, G.F.; Tan, W.; Ph.D. for the China Novel Coronavirus Investigating and Research Team. A Novel Coronavirus from Patients with Pneumonia in China, 2019. *N. Engl. J. Med.* **2020**, *382*, 727-733, https://doi.org/10.1056/NEJMoa2001017.
4. Lassoued, A.; Saad, A.B.; Lassoued, H.; Ketata, R.; Boubaker, O. Dataset on the COVID-19 Pandemic Situation in Tunisia with application to SIR Model. *medRxiv* **2020**, https://doi.org/10.1101/2020.04.23.20076802.

5. Choy, K.-T.; Wong, A.Y.-L.; Kaewpreedee, P.; Sia, S.F.; Chen, D.; Hui, K.P.Y.; Chu, D.K.W.; Chan, M.C.W.; Cheung, P.P.-H.; Huang, X.; Peiris, M.; Yen, H.-L. Remdesivir, lopinavir, emetine, and homoharringtonine inhibit SARS-CoV-2 replication in vitro. *Antivir. Res.* **2020**, *178*, 104786, https://doi.org/10.1016/j.antiviral.2020.104786.
6. Jin, Z.; Du, X.; Xu, Y.; Deng, Y.; Liu, M.; Zhao, Y.; Zhang, B.; Li, X.; Zhang, L.; Peng, C.; Duan, Y.; Yu, J.; Wang, L.; Yang, K.; Liu, F.; Jiang, R.; Yang, X.; You, T.; Liu, X.; Yang, X.; Bai, F.; Liu, H.; Liu, X.; Guddat, L.W.; Xu, W.; Xiao, G.; Qin, C.; Shi, Z.; Jiang, H.; Rao, Z.; Yang, H. Structure of M^{pro} from SARS-CoV-2 and discovery of its inhibitors. *Nature* **2020**, *582*, 289-293, https://doi.org/10.1038/s41586-020-2223-y.
7. Shah, B.; Modi, P; Sagar, S.R. *In silico* studies on therapeutic agents for COVID-19: Drug repurposing approach. *Life Sci.* **2020**, *252*, 117652, https://doi.org/10.1016/j.lfs.2020.117652.
8. Brown, A.J.; Won, J.J.; Graham, R.L.; Dinnon III, K.H.; Sims, A.C.; Feng, J.Y.; Cihlar, T.; Denison, M.R.; Baric, R.S.; Sheahan, T.P. Broad spectrum antiviral remdesivir inhibits human endemic and zoonotic deltacoronaviruses with a highly divergent RNA dependent RNA polymerase. *Antivir. Res.* **2019**, *169*, 104541, https://doi.org/10.1016/j.antiviral.2019.104541.
9. Glaus, M.J.; Von Ruden, S. Remdesivir and COVID-19. *Lancet* **2020**, *396*, 952, https://doi.org/10.1016/S0140-6736(20)32021-3.
10. COVID, A., 19. Treatment Trial. ClinicalTrials. gov identifier: NCT04280705. Posted February 21, **2020**.
11. Wang, M.; Cao, R.; Zhang, L.; Yang, X.; Liu, J.; Xu, M.; Shi, Z.; Hu, Z.; Zhong, W.; Xiao, G. Remdesivir and chloroquine effectively inhibit the recently emerged novel coronavirus (2019-nCoV) in vitro. *Cell Res.* **2020**, *30*, 269-271, https://doi.org/10.1038/s41422-020-0282-0.
12. Blanchard, J.E.; Elowe, N.H.; Huitema, C.; Fortin, P.D.; Cechetto, J.D.; Eltis, L.D.; Brown, E.D. High-Throughput Screening Identifies Inhibitors of the SARS Coronavirus Main Proteinase. *Chem. Biol.* **2004**, *11*, 1445-1453, https://doi.org/10.1016/j.chembiol.2004.08.011.
13. Chu, C.M.; Cheng, V.C.C.; Hung, I.F.N.; Wong, M.M.L.; Chan, K.H.; Chan, K.S.; Kao, R.Y.T.; Poon, L.L.M.; Wong, C.L.P.; Guan, Y.; Peiris, J.S.M.; Yuen, K.Y.Y. Role of lopinavir/ritonavir in the treatment of SARS: initial virological and clinical findings. *Thorax* **2004**, *59*, 252-256, http://dx.doi.org/10.1136/thorax.2003.012658.
14. Lu, I.-L.; Mahindroo, N.; Liang, P.-H.; Peng, Y.-H.; Kuo, C.-J.; Tsai, K.-C.; Hsieh, H.-P.; Chao, Y.-S.; Wu, S.-Y. Structure-Based Drug Design and Structural Biology Study of Novel Nonpeptide Inhibitors of Severe Acute Respiratory Syndrome Coronavirus Main Protease. *J. Med. Chem.* **2006**, *49*, 5154-5161, https://doi.org/10.1021/jm060207o.
15. Banerjee, R.; Perera, L.; Tillekeratne, L.M.V. Potential SARS-CoV-2 main protease inhibitors. *Drug Discov. Today* **2021**, *26*, 804-816, https://doi.org/10.1016/j.drudis.2020.12.005.
16. Zumla, A.; Chan, J.F.W.; Azhar, E.I.; Hui, D.S.C.; Yuen, K.-Y. Coronaviruses - drug discovery and therapeutic options. *Nat. Rev. Drug Discov.* **2016**, *15*, 327-347, https://doi.org/10.1038/nrd.2015.37.
17. Anderson, A.C. The Process of Structure-Based Drug Design. *Chem. Biol.* **2003**, *10*, 787-797, https://doi.org/10.1016/j.chembiol.2003.09.002.
18. Ferreira, L.G.; Dos Santos, R.N.; Oliva, G.; Andricopulo, A.D. Molecular Docking and Structure-Based Drug Design Strategies. *Molecules* **2015**, *20*, 13384-13421, https://doi.org/10.3390/molecules200713384.
19. Abdolmaleki, A.; Ghasemi, J.B.; Ghasemi, F. Computer Aided Drug Design for Multi-Target Drug Design: SAR /QSAR, Molecular Docking and Pharmacophore Methods. *Curr. Drug Targets* **2017**, *18*, 556-575, http://doi.org/10.2174/1389450117666160101120822.
20. Mwine, J.T.; Van Damme, P. Why do Euphorbiaceae tick as medicinal plants? A review of Euphorbiaceae family and its medicinal features. *J. Med. Plant Res.* **2011**, *5*, 652-662.
21. Poyil, M.M.; Karrar Alsharif, M.H.; Seshadri, V.D. Anti-asthmatic activity of Saudi herbal composites from plants *Bacopa monnieri* and *Euphorbia hirta* on Guinea pigs. *Green Process. Synth.* **2022**, *11*, 512-525, https://doi.org/10.1515/gps-2022-0039.
22. Aqil, M. Euphorbianin, a New Glycoside from Euphorbia hirta Linn. *Global J. Pure Appl. Sci.* **1999**, *5*, 371-374.
23. Yusuf, M.; Wahab, M.A.; Yousuf, M.; Chowdhury, J.U.; Begum, J. Some tribal medicinal plants of Chittagong Hill Tracts, Bangladesh. *Bangladesh J. Plant Taxon.* **2007**, *14*, 117-128, https://doi.org/10.3329/bjpt.v14i2.531.
24. Parmar, G.R.; Pundarikakshudu, K. Comparative Pharmacognostic and Phytochemical Standardization of Euphorbia hirta L. and Euphorbia thymifolia L. *Am. J. PharmTech Res.* **2017**, *7*, 531-544.

25. Huang, L.; Chen, S.; Yang, M. Euphorbia hirta (Feiyangcao): A review on its ethnopharmacology, phytochemistry and pharmacology. *J. Med. Plant Res.* **2012**, *6*, 5176-5185, https://doi.org/10.5897/JMPR12.206.
26. Ernst, E. Phytotherapy: A quick reference to herbal medicine. *Phytomedicine*: *Int. J. Phytother. Phytopharmacol.* **2004**, *11*, 557.
27. Shah, A.P.; Parmar, G.R.; Sailor, G.U.; Seth, A.K. Antimalarial Phytochemicals Identification from *Euphorbia Hirta* against Plasmepsin Protease: an *In Silico* Approach. *Folia Med.* **2019**, *61*, 584-593, https://doi.org/10.3897/folmed.61.e47965.
28. Berman, H.M.; Westbrook, J.; Feng, Z.; Gilliland, G.; Bhat, T.N.; Weissig, H.; Shindyalov, I.N.; Bourne, P.E. The Protein Data Bank. *Nucleic Acids Res.* **2000**, *28*, 235-242, https://doi.org/10.1093/nar/28.1.235.
29. Dallakyan, S.; Olson, A.J. Small-Molecule Library Screening by Docking with PyRx. In Chemical Biology. Methods in Molecular Biology, Hempel, J.; Williams, C.; Hong, C., Eds.; Humana Press, New York, NY, **2015**, Volume 1263, 243-250, https://doi.org/10.1007/978-1-4939-2269-7_19.
30. Zochedh, A.; Chandran, K.; Priya, M.; Sultan, A.B.; Kathiresan, T. Molecular simulation of naringin combined with experimental elucidation–Pharmaceutical activity and Molecular docking against Breast cancer. *J. Mol. Struct.* **2023**, *1285*, 135403, https://doi.org/10.1016/j.molstruc.2023.135403.
31. Priya, M.; Zochedh, A.; Arumugam, K.; Sultan, A.B. Quantum Chemical Investigation, Drug-Likeness and Molecular Docking Studies on Galangin as Alpha-Synuclein Regulator for the Treatment of Parkinson's Disease. *Chem. Afr.* **2023**, *6*, 287-309, https://doi.org/10.1007/s42250-022-00508-z.
32. Pashmforosh, M.; Shariati, S.; Nezhad, H.A.; Haghighat, M. Possible Benefits of Paclitaxel Therapy for COVID-19. *Pharm. Biomed. Res.* **2022**, *8*, 91-94, http://doi.org/10.18502/pbr.v8i2.11022.
33. Sukumaran, S.; Zochedh, A.; Viswanathan, T.M.; Sultan, A.B.; Kathiresan, T. Theoretical Investigation of 5-Fluorouracil and Tamoxifen Complex – Structural, Spectrum, DFT, ADMET and Docking Simulation. *Polycycl. Aromat. Compd.* **2023**, *43*, 9443-9460, https://doi.org/10.1080/10406638.2022.2164018.
34. Priya, M.; Arumugam, K.; Chakaravarthy, C.; Chandran, K.; Sultan, A.B.; Zochedh, A. Graph Theory Network, Molecular Docking, Quantum Chemicals and Pharmacokinetics-Based Investigation on Phytochemicals from *Sida rhombifolia* against Alzheimer's Disease. *Polycycl. Aromat. Compd.* **2023**, 1-24, https://doi.org/10.1080/10406638.2023.2209259.
35. Zochedh, A.; Chandran, K.; Shunmuganarayanan, A.; Sultan, A.B. Exploring the Synergistic Effect of Tegafur-Syringic Acid Adduct Against Breast Cancer through DFT Computation, Spectroscopy, Pharmacokinetics and Molecular Docking Simulation. *Polycycl. Aromat. Compd.* **2023**, 1-35, https://doi.org/10.1080/10406638.2023.2214281.
36. Chandran, K.; Zochedh, A.; Sultan, A.B.; Kathiresan, T. Observations into quantum simulation, spectroscopy, electronic properties, pharmacokinetics and molecular docking analysis of lawsone against breast cancer. *J. Mol. Struct.* **2023**, *1293*, 136280, https://doi.org/10.1016/j.molstruc.2023.136280.
37. Zochedh, A.; Chandran, K.; Priya, M.; Sultan, A.B.; Kathiresan, T. DFT Simulation of Berberine Chloride with Spectroscopic Characterization–Biological activity and Molecular Docking against Breast Cancer. *Polycycl. Aromat. Compd.*, **2023**, 1-25, https://doi.org/10.1080/10406638.2023.2201457.
38. Priya, M.; Zochedh, A.; Palaniyandi, K.; Shunmuganarayanan, A.; Sultan, A.B. Combinatorial Effect of Syringic Acid-Pyrazinamide Adduct against Luminal Type Breast Cancer Investigated through DFT, Drug-Likeness, and Molecular Docking Simulation. *Polycycl. Aromat. Compd.* **2023**, 1-29, https://doi.org/10.1080/10406638.2023.2212105.